

1 **Critical evaluation of aptamer binding for biosensor designs**

2
3 Yichen Zhao, Kayvan Yavari and Juewen Liu*

4 Department of Chemistry, Waterloo Institute for Nanotechnology, University of Waterloo,
5 Waterloo, Ontario, N2L 3G1, Canada

6 Email: liujw@uwaterloo.ca

7
8 **Abstract**

9 Over the last three decades, numerous aptamer-based biosensors have been reported. The basis of
10 these sensors is the selective binding of target analytes by aptamers. In the last few years, a number
11 of papers have been published questioning the binding ability of some popular aptamers such as
12 those documented for As(III), ampicillin, chloramphenicol, isocarboxiphos, phorate and dopamine.
13 In this article, these papers are reviewed, and the binding assays are described, which may provide
14 possible reasons for obtaining false positive aptamers. Additionally, relevant aptamer selection
15 methods and typical characterization steps are also described. It is found that for small molecular
16 targets, using an immobilized library might result in better aptamers. Furthermore, the importance
17 of carefully designed controls to ensure the quality of binding assays is discussed, especially in the
18 case of mutated nonbinding aptamers. Only then, with fully validated aptamers, can subsequent
19 biosensor design bring about meaningful results.

20
21 **Keyword:** aptamers; dissociation constant; biosensors; isothermal titration calorimetry; SELEX

23 **Introduction**

24 Aptamers are single-stranded oligonucleotides that can selectively bind to target molecules. Since
25 their first report in 1990 [1, 2], aptamers have been widely used for target recognition in biosensor
26 development [3-8]. Compared to antibodies, DNA aptamers are much more stable, and can be
27 better adapted for site-specific labeling. More importantly, aptamers have programmable
28 structures and can switch between states of free aptamers, target binding, and binding of
29 complementary DNA. Their versatility allows for a diverse range of signal transduction methods
30 from optical to electrochemical detection [9]. Another advantage of aptamers is that they are
31 particularly useful for binding small molecular targets [10, 11]. In fact, most riboswitches
32 (aptamers in the untranslated regions of mRNA for regulating gene expression) bind to small
33 molecules or ions [12].

34 A few classic aptamers such as those that bind to ATP [13], cocaine [14], and thrombin
35 [15] have been extensively studied and used as model systems for demonstrating various sensing
36 methods. Most of the early aptamer selection work was performed by biochemists, hence the
37 reported aptamers were subjected to stringent biochemical characterizations such as binding
38 affinity assays, secondary structure analysis, mutation of critical nucleotides, and binding of
39 closely related target analogs.

40 That said, aptamer selection is a fairly straightforward process, accessible to most labs with
41 a PCR thermocycler. Encouraged by past success, more researchers have joined the force of
42 aptamer selection in order to solve problems in their respective fields. To date, hundreds of
43 aptamers have been published. However, while following an aptamer selection process always
44 results in DNA sequences, the obtained sequences are not necessarily true aptamers. Evaluation of
45 aptamer binding is a challenging task [16-18]. Without appropriate controls, non-aptamer
46 sequences might show false positive binding results. Sensors designed using these sequences
47 would then, not give reliable analytical results.

48 Over the last five years, quite a few papers have begun to question some previously claimed
49 aptamer sequences, and we intended to summarize them here. In this review paper, we focus on
50 aptamers for small molecules. The methods of selection and characterization are described in each
51 example along with our own critical evaluation. In the end, possible reasons for generating such

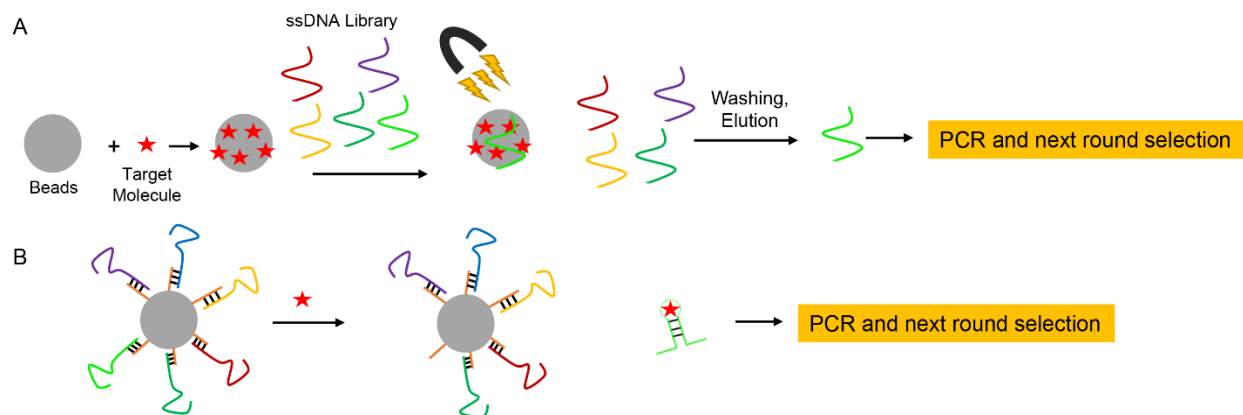
52 non-aptamer sequences and their use in biosensors are discussed. Future work to address these
53 problems is also proposed.

54 **Aptamer selection**

55 Most DNA libraries for aptamer selection contain a random region (typically 20 to 60 nucleotides)
56 flanked with two constant regions for binding of PCR primers. Following the incubation of a
57 library with target analytes, the binding sequences are then separated from the non-binding ones.
58 For small molecular targets, either target immobilization or DNA library immobilization can be
59 used to achieve sequence discrimination. Early works employed the target immobilization method
60 by covalently linking target molecules to a solid surface such as agarose or magnetic beads (Figure
61 1A). In this way, the non-binding sequences were washed away. Finally, the binding sequences
62 were eluted and amplified by PCR. This method has generated many classic aptamers and
63 continues to be used to date [5, 10].

64 Nevertheless, not all target molecules can be covalently immobilized. In addition,
65 immobilization would unavoidably block part of molecules, making it inaccessible to DNA
66 binding. The effects of immobilization are more adverse for smaller molecules and are extreme
67 for metal ions. The alternative idea of library immobilization was inspired by the structure-
68 switching property of aptamers reported by the Li group [19, 20]. The same group also
69 demonstrated the library immobilization method for aptamer selection [21]. This method was later
70 used by many other groups such as Ellington [22], Stojanovic [23, 24], and Xiao [25, 26]. The idea
71 is to immobilize a DNA library via DNA hybridization, and it is also called capture-SELEX [27].
72 The library is often designed to have a hairpin structure. Aptamer sequences bind to targets to form
73 hairpins are released and collected. This method can be applied to any target molecule. The hairpin
74 structure also makes subsequent truncation and secondary structure analysis much more efficient.

75 Typically, due to non-specific DNA binding or non-specific DNA dissociation, more than
76 ten rounds of selection are required to obtain high quality aptamers using either method [5, 10]. If
77 at the end of a selection, non-specific processes still dominate, the selection might result in non-
78 specific DNA sequences in the final library. Therefore, whether the obtained sequences are real
79 aptamers needs to be carefully characterized.



80
 81 **Figure 1.** Illustrations showing two types of aptamer selection methods. (A) The target
 82 immobilization method. (B) The library immobilization method, where a hairpin structure is
 83 designed in the library sequence.

84
 85 **Aptamer characterization**

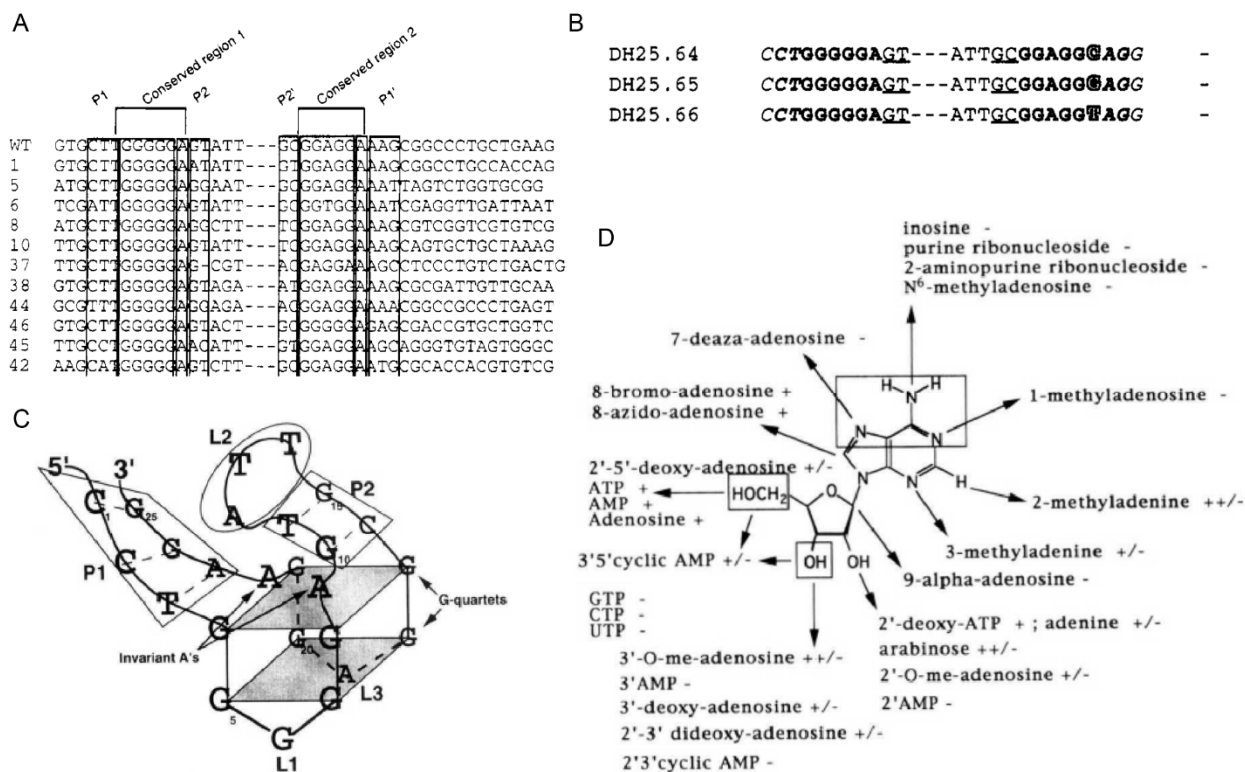
86 After selection and sequencing of the final library, the obtained sequences are typically
 87 characterized using biochemical assays. The relevant steps are illustrated by an example of the
 88 classic ATP aptamer first isolated by Huizenga and Szostak in 1995 [13]. Following the
 89 sequencing of the library, the first step would be to align the sequences. Cloning following Sanger
 90 sequencing typically produces less than 100 sequences. A portion of the aligned random region of
 91 the ATP aptamer selection is shown in Figure 2A, where two highly conserved regions have been
 92 identified. In addition, base covariation was observed in two other regions, suggesting base pairing.
 93 Sequences outside these regions were highly variable. This is a good indication of a successful
 94 selection. If the obtained sequences cannot be aligned at all, it is unlikely that the final library can
 95 specifically bind to target molecules, since it is unlikely that DNA can have numerous distinct
 96 ways to bind to a molecule. Currently, direct sequencing of PCR products using deep sequencing
 97 technologies can easily produce over 30,000 sequences [28]. Nevertheless, similar methods of
 98 sequence alignment need also to be carried out.

99 The importance of each nucleotide in the conserved region can be studied via mutations.
 100 For example, Figure 2B shows the mutation of an adenine to the other three nucleotides
 101 respectively, and in each case, the subsequent binding activity was lost. This experiment indicates

102 not only the importance of this adenine for target binding, but also demonstrates its importance to
103 specific binding. If all the nucleotides can be mutated and the binding is still measurable, then
104 likely the binding assay cannot probe specific binding, or the sequence is not an aptamer, or both.
105 Such inactive mutants are also highly useful for confirmation of sensor design, as sensors based
106 on inactive mutants should not give the same signals as aptamers. Mutation studies may also help
107 construct secondary structures. In the original paper, the predicted secondary structure is shown in
108 Figure 2C. Although later, NMR studies disproved the G-quadruplex based structure [29], the
109 general hairpin structure with a short stem is proven correct in the end. For most biosensor
110 applications, information on the overall hairpin structure would already be quite helpful.

111 Binding assays are critical to characterize aptamers. A few papers and reviews have already
112 been published on this topic and thus they will not be repeated here [5, 16, 17]. However, in the
113 next sections while discussing individual examples, we will touch on some relevant binding assays.
114 Finally, a further characterization is the test of analogs of target molecules. In this particular ATP
115 aptamer paper, extensive studies have been performed (Figure 2D). This information is useful for
116 biosensors in terms of target selectivity.

117 However, many of these steps were not consistently performed for all the selected aptamers;
118 skipping these steps may have resulted in non-aptamer sequences being reported as aptamers. For
119 analytical chemists, it is also important to see if such characterization work has been done
120 previously. If not, then control experiments would be even more important, such as the use of non-
121 binding mutants, and performance of independent binding assays. In the following sections, five
122 examples from the recent literatures are discussed, each questioning one or two aptamers.



123

124 **Figure 2.** Analysis of the ATP binding aptamer selection results. (A) A portion of the sequence
 125 alignment results. The numbers on the left can be considered as the names of the sequences.
 126 Covariation of P1/P1' and P2/P2' suggests their base pairing. (B) Mutating an adenine base to G,
 127 C or T all abolished binding. (C) A proposed secondary structure of the aptamer. Although later
 128 studies disproved the G-quadruplex structure, the closing of the two ends which form a stem is
 129 proven correct. (D) Some analogs tested for binding with the aptamer (“+” indicates good binding,
 130 while “-” indicates no binding). Figures adapted from ref [13]. with permission. Copyright 1995
 131 American Chemical Society.

132

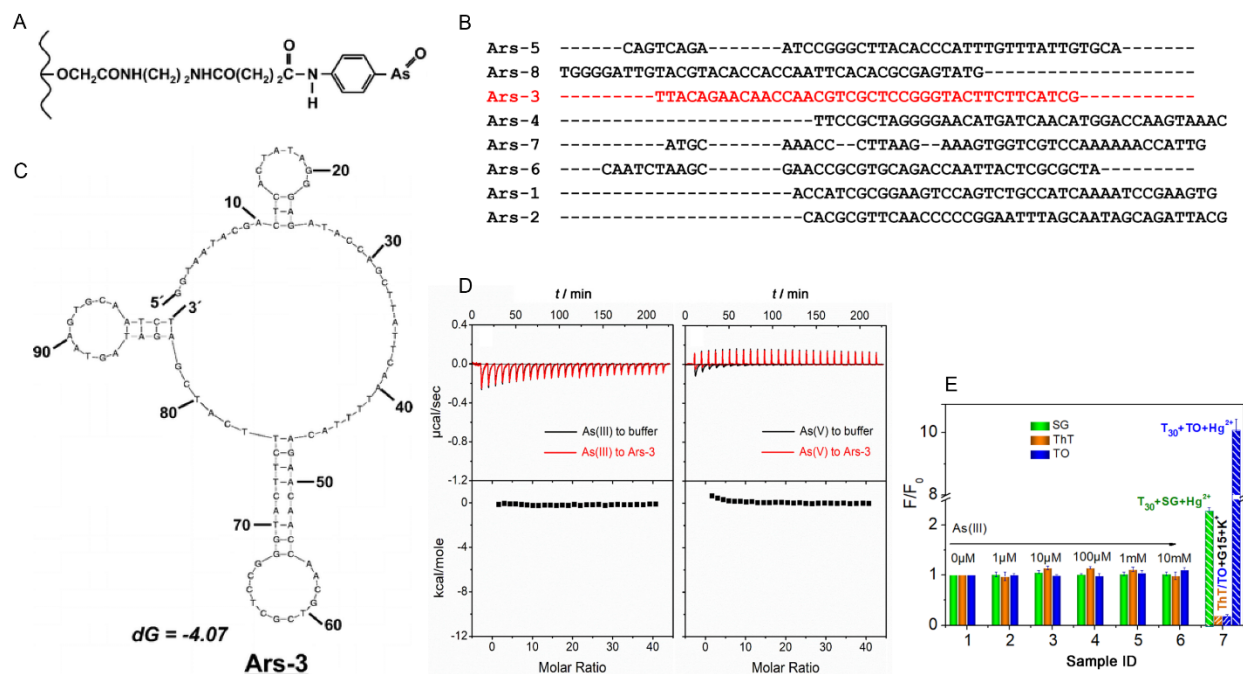
133 **Arsenic**

134 Arsenic is a highly important element for environmental analytical chemistry [30-33]. An arsenic
 135 binding aptamer named Ars-3 was reported in 2009 for the purpose of removing arsenic from water
 136 [34]. The aptamer selection was performed by conjugating phenylarsine oxide on a gel resin
 137 surface (Figure 3A). While the oxidation state of the immobilized arsenic was +3, its chemical
 138 property is likely to have been different from that of inorganic arsenite (AsO₂⁻) due to the bonding

139 with a benzyl ring. After 10 rounds of selection, the library was sequenced. Out of the 40 sequences,
140 Ars-3 was the most abundant, appearing 12 times. The next most abundant sequences appeared 7
141 times or less. We took the reported sequences and aligned them using Clustal Omega [35].
142 However, it was hard to find two sequences with highly conserved regions (Figure 3B).

143 The binding was characterized using surface plasmon resonance (SPR) on a gold surface,
144 where As(III) and As(V) were covalently linked [34]. The binding of the aptamer was expected to
145 create a shift in the SPR signal. The best aptamer was found to be Ars-3 (Figure 3C), which had a
146 similar binding affinity for As(III) (5 nM) and As(V) (7 nM). Since the selection was performed
147 with As(III), and given the chemical difference between these two arsenic oxidation states, it is
148 hard to understand why the aptamer appeared to bind both. We suspected that the measured binding
149 could be due to the adsorption of the DNA to the gold surface, since DNA bases have strong
150 affinities to gold [36, 37]. This aptamer has since been used for designing various biosensors for
151 the detection of arsenic. Although the original aptamer claimed to bind both As(III) and As(V),
152 most of the sensor work could only detect As(III) [38-40].

153 In most of the follow-up papers, the entire 100-nt sequence was used without truncation.
154 For an aptamer that binds to such a small target and given its predicted secondary structure (Figure
155 3C), it is unlikely that the entire sequences would be needed. Very recently, a truncated sequence
156 was reported by taking the 21-mer sequence from nucleotide number 80 to 100 (Figure 3C) [41].
157 However, these nucleotides belonged to the fixed region of the library and are therefore unlikely
158 to be able to bind As(III). For the truncated sequence, the main evidence of binding was from a
159 change of the CD spectra upon adding As(III), although no control DNA sequences were tested.
160 Some of these doubts led us to carefully examine the binding of this aptamer. Using isothermal
161 titration calorimetry (ITC), we obtained no sign of binding of either As(III) or As(V) (Figure 3C)
162 [35]. In addition, we used a few DNA staining dyes to probe DNA structural changes, such as
163 SYBR Green I (SG) to probe duplex, thioflavin T (ThT) to probe G-quadruplex, and thiazole
164 orange (TO) to probe both duplex and G-quadruplex [42, 43]. If aptamer binding occurs, the dyes
165 can either be displaced by the target or sometimes enhanced binding can occur, both of which may
166 influence the fluorescence intensity. However, none of them showed much fluorescence change
167 upon adding up to 1 mM As(III) (Figure 3D). On the other hand, large changes were observed with
168 the positive control DNA sequences by adding Hg^{2+} or K^+ .



169

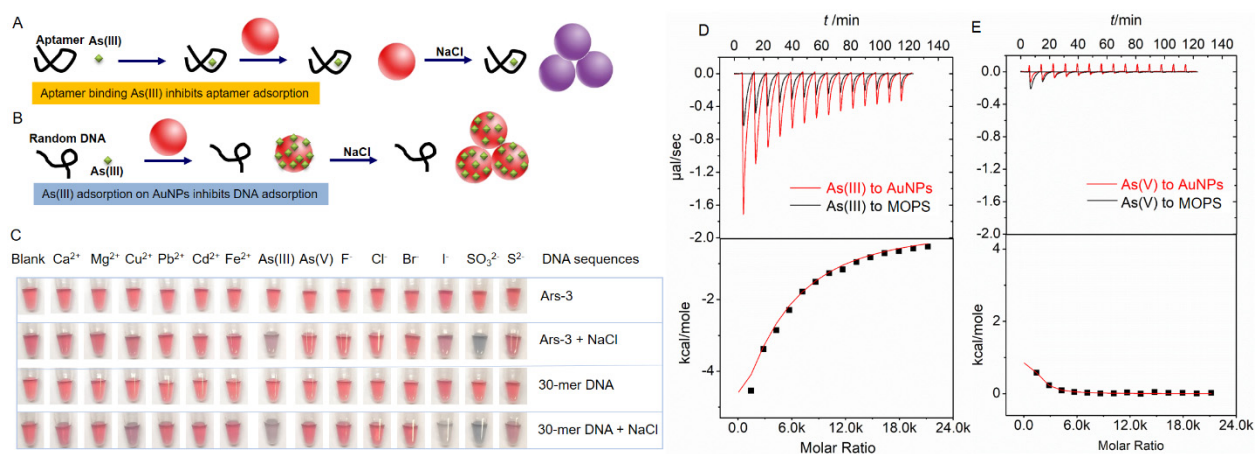
170 **Figure 3.** (A) The immobilized arsenic species used for the aptamer selection. (B) The alignment
 171 of selected DNA sequences. (C) The predicted secondary structure of the Ars-3 sequence. (D) ITC
 172 traces and integrated heat of As(III) and As(V) titration into the Ars-3. (E) Fluorescence change
 173 upon adding various concentrations of As(III) to Ars-3 in the presence of three different DNA
 174 staining dyes. Group 7 comprised positive controls using T_{30} with Hg^{2+} , or G_{15} DNA with K^+ . (A,
 175 C) Adapted from ref. [34] with permission. Copyright 2009 American Chemical Society. (B, D,
 176 E) Adapted from ref. [35] with permission. Copyright 2019 American Chemical Society.

177

178 To understand why the many reported sensors were able to detect As(III) with Ars-3, we
 179 studied the literature in detail and found that quite a few papers used gold nanoparticles (AuNPs)
 180 to develop colorimetric sensors [38-40, 44]. Although each work has a different design, the general
 181 idea for the simplest system is described in Figure 4A. Once As(III) binds to the aptamer, the
 182 aptamer would fold into a compact structure, preventing it from adsorbing onto the AuNPs. Upon
 183 adding salt, the non-protected AuNPs were aggregated leading to a red-to-blue color change. This
 184 method was originally used for the detection of complementary DNA [45, 46]. Since DNA binds
 185 to its complementary strand with a very high affinity, few free target DNA would be present in the
 186 system. For aptamer-based detection, however, the potential interactions between target analytes

187 and AuNPs has not been considered [18, 47]. We suspected that another mechanism might also be
 188 possible (Figure 4B) [48], in which the added As(III) can adsorb onto AuNPs. The adsorbed As(III)
 189 would then inhibit the adsorption of DNA. Since the AuNPs were not protected by the DNA,
 190 adding salt would yield a blue color. Although the final color change was the same, the
 191 mechanisms were very different. In Figure 4B, any DNA sequence would have a similar result.
 192 This was indeed what we observed (Figure 4C), where the As(III) containing samples turned blue
 193 regardless of whether the aptamer or a random 30-mer DNA was used. The papers also tested a
 194 few control analytes such as As(V) and metal cations. These metal cations resulted in red color
 195 since they cannot adsorb onto AuNPs and would not inhibit DNA adsorption. We also tested a few
 196 anions, and many with strong affinities to gold also resulting in blue color (Figure 4C). To confirm
 197 As(III) adsorption onto AuNPs, we performed ITC and only As(III) (Figure 4D) but not As(V)
 198 (Figure 4E) showed adsorption.

199 Therefore, we believe that many of the papers using Ars-3 detected As(III) adsorption by
 200 AuNPs instead of detecting As(III) binding to the aptamer. In addition, gold surfaces were also
 201 used to interface with Ars-3 and its derived sequences for developing electrochemical sensors [49],
 202 piezoelectric sensors [50], SERS sensors [51, 52], fluorescence dequenching sensors [53], and SPR
 203 sensors [34]. These sensors might also be affected by the adsorption of As(III) to their gold
 204 surfaces.



205
 206 **Figure 4.** Schemes demonstrating two mechanisms of aptamer and AuNP based As(III) detection,
 207 where (A) relies on the aptamer binding to As(III), and (B) relies on As(III) adsorption onto AuNPs.
 208 Adapted from ref. [48] with permission. Copyright 2019 American Chemical Society. (C)
 209 Photographs showing the color of AuNPs in the presence of various ions with Ars-3 or a random

210 30-er DNA. After adding NaCl, the As(III) containing samples both turned blue. ITC traces of
211 titrating (D) As(III), and (E) As(V) into AuNPs. Adapted from ref. [35] with permission. Copyright
212 2019 American Chemical Society.

213

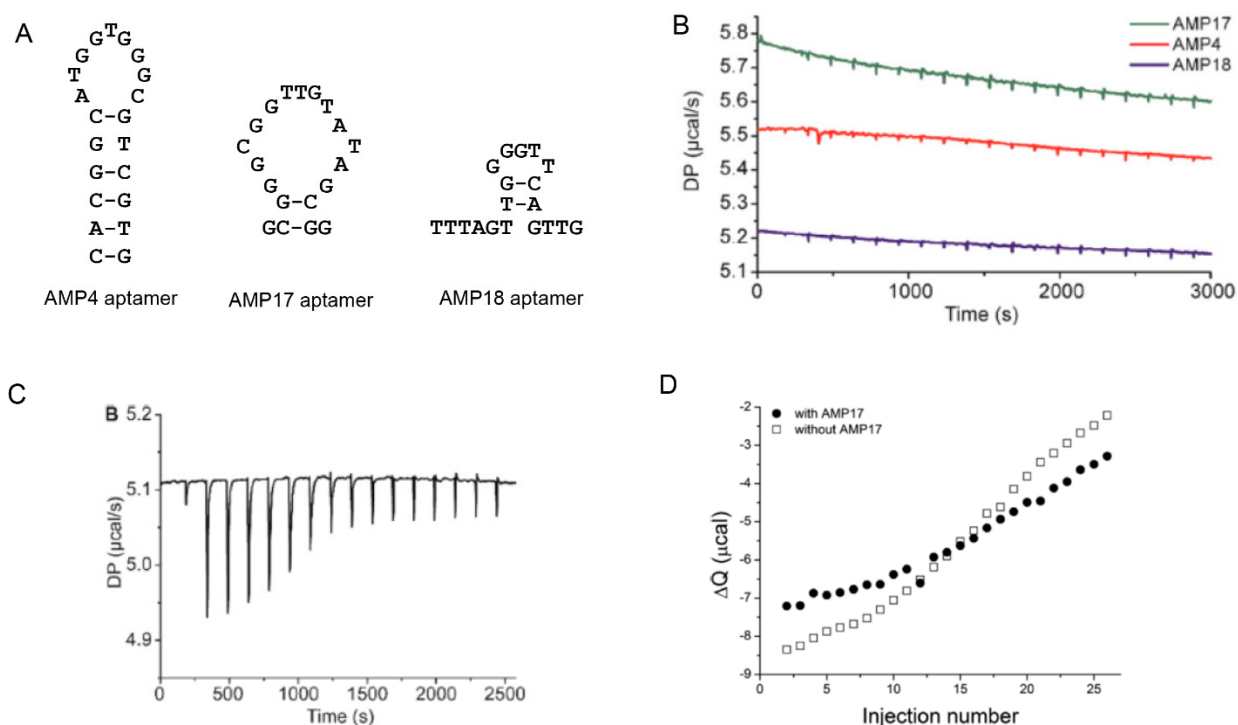
214 **Ampicillin**

215 Ampicillin is a member of the beta-lactam family of antibiotics and is commonly used to treat both
216 humans and animals. The misuse and overuse of ampicillin has caused residues to be left in food
217 products which have been shown to lead to health complications such as allergies, seizures and
218 breathing difficulties in humans. Aptamers were selected for ampicillin using the target
219 immobilization method, where ampicillin was immobilized on tosyl-activated magnetic beads [54].
220 After 13 rounds of selection, three aptamers were obtained (AMP4, AMP17, AMP18, Figure 5A)
221 with dissociation constants of 9.4, 13.4 and 9.8 nM respectively. Their K_d values were determined
222 using FAM-labeled aptamers incubated with ampicillin immobilized beads, the fluorescence
223 intensities of which were measured at various concentrations of the aptamer. To prove the sensing
224 characteristics of the resulting aptamers, colorimetric AuNP-based assays were performed similar
225 to that described in Figure 4A. However, this type of assay is not always accurate, especially when
226 target analytes can interact with AuNPs.

227 A recent study by Bottari et al. aimed to take a closer look at the actual binding between
228 ampicillin and the three aptamers by using ITC. The results were then compared to two other well
229 characterized aptamers, the cocaine/quinine binding aptamer (MN4) [55], and the L-argininamide
230 (1OLD) [56]. The corresponding ITC thermographs show no binding events related to ampicillin
231 when the aptamers were titrated (Figure 5B). Compared to the ITC thermographs of MN4 when
232 titrated with quinine (Figure 5C), there is a clear lack of thermal binding events between ampicillin
233 and its aptamers. Due to the type of assay used to evaluate the binding characteristics (AuNP assay),
234 interactions between the AuNPs and ampicillin itself were also evaluated (Figure 5D). A clear
235 indication of interactions between AuNPs and ampicillin was observed, while adding an aptamer
236 had little effect. We suspected that the change of AuNP color was mainly driven by the adsorption
237 of ampicillin, just like in the case of the As(III) example described above. This is not the first time
238 that the interaction between antibiotics and AuNPs in a colorimetric assay interfered with the
239 results of sensing. Another study for the detection of kanamycin showed that the color of the

240 AuNPs changed regardless of the sequence of DNA used [57]. Therefore, extra care should be
241 taken to ensure that there is minimal interaction between target molecules and AuNPs. Otherwise,
242 such an assay cannot be used.

243 Aside from ITC, the authors also used native nano-electrospray ionization mass
244 spectrometry and proton NMR to measure the binding between ampicillin and its aptamers. These
245 techniques were chosen since they could probe K_d values in different regions. However, neither
246 methods indicated specific binding of these aptamers. Therefore, these assays collectively
247 disproved these sequences as aptamers for ampicillin [58].



248
249 **Figure 5.** (A) Sequence and secondary structures of AMP4, AMP17, and AMP18 [45, 59]. (B)
250 ITC traces of AMP17, AMP4, AMP18 titrated with 280 μM ampicillin. (C) ITC traces of the MN4
251 aptamer titrated with 50 μM quinine. (D) Heat generated from each injection of titrating ampicillin
252 into AuNP with AMP17 (full dots) and AuNPs alone (empty squares). Figures adapted from ref.
253 [58] with permission. Copyright 2020 American Chemical Society.

254

255 Chloramphenicol

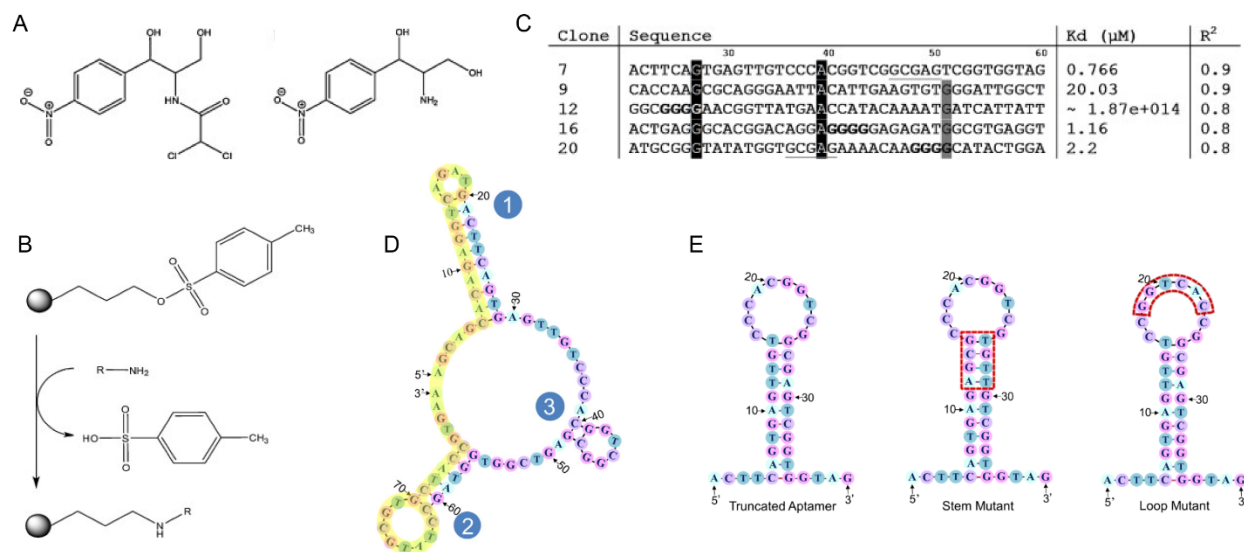
256 Chloramphenicol (CAP) is a potent antibiotic, but it was banned in the EU, USA, and China due
257 to its side-effects which lead to leukemia, aplastic anemia, and grey baby syndrome [60]. However,
258 its illicit use continues to date. CAP has an overall neutral charge (Figure 6A, left side). Based on
259 its structure, it has hydrogen bonding donors/acceptors, as well as potential charge, pi-pi stacking
260 and hydrophobic interactions with DNA. Therefore, it should be a good target for aptamer binding.
261 In 2011, an aptamer selection was performed by immobilizing the structure on the right side of
262 Figure 6A on magnetic beads via the primary amine group (Figure 6B) [61]. Compared to CAP,
263 however, the immobilized molecule did not have the two chlorine atoms.

264 The round 8 library was cloned and sequenced, a few sequences of which are shown in
265 Figure 6C. The K_d values were measured based on binding to the magnetic beads of selection.
266 Although free CAP was also used as a binding assay, this assay still relied on the beads as
267 competitors. The fraction of aligned sequences seemed to be low, and the underlined conserved
268 regions appeared in distinct parts of the secondary structure. The as-selected CAP aptamers were
269 80-nt, and one sequence was predicted to fold in a structure with two hairpins linked by a large
270 loop (Figure 6D). No truncation study was performed in the original selection work [61], and more
271 rigorous binding assays such as ITC have yet to be carried out. A few subsequent biosensor works
272 also used this full 80-nt sequence [62, 63].

273 The first truncation of this CAP aptamer was reported in 2014, which simply deleted the
274 20-nt segments on both the 3' and the 5' sides, leaving only the 40-nt in the middle (Figure 6E,
275 left) [64]. However, little rigorous binding assays were performed on this truncated aptamer. By
276 simply examining the predicted secondary structures, such truncation would completely disrupt
277 the two original stem-loops, resulting in a distinct secondary structure. We reasoned that if the
278 CAP binding pockets resided in regions 1, 2 or 3, or a combinations, (Figure 6D) none of these
279 features would be left from the original aptamer after the truncation [65]. Regions 1 and 2 were
280 fully disrupted, whereas region 3 was folded into a stable hairpin. Therefore, by simply examining
281 the structures, it is unlikely that the truncated sequence could retain the same binding mechanism
282 as the original aptamer. Nevertheless, this truncated sequence has since gained popularity for
283 biosensor design, which has likely been due to its shorter length.

284 We continued by performing ITC and DNA staining dye-based fluorescence spectroscopy,
285 but none of them demonstrated the binding of the truncated aptamer. Thus, we do not believe that

286 this truncated sequence is a real aptamer [65]. Whether the original 80-nt one is a real aptamer or
 287 not still requires more stringent studies.



288
 289 **Figure 6.** (A) The structure of CAP (left), and the molecule used for immobilization (right). (B)
 290 The chemistry of target immobilization. (C) Aptamer sequence alignment. Figures adapted from
 291 ref. [61] with permission. Copyright 2011 Elsevier. The predicted secondary structures of (D) the
 292 original 80-nt aptamer divided in three regions, (E) the truncated 40-nt aptamer, and the two
 293 control sequences with the four highlighted base pairs in the stem in the switched position (Stem
 294 Mutant), and mutations in the loop (Loop Mutant). Figures adapted from ref. [65] with permission.
 295 Copyright 2020 Springer.

296

297 Isocarbophos and phorate

298 Pesticides are commonly used in agriculture and have been documented to contaminate both food
 299 production as well as the environment. Organophosphorus pesticides are the most commonly used
 300 class of pesticides. They can cause adverse health problems in humans, posing a serious risk to
 301 public health. As a result, there has been an increasing interest for the selection of aptamers and
 302 the development of aptasensors for these pesticides [66].

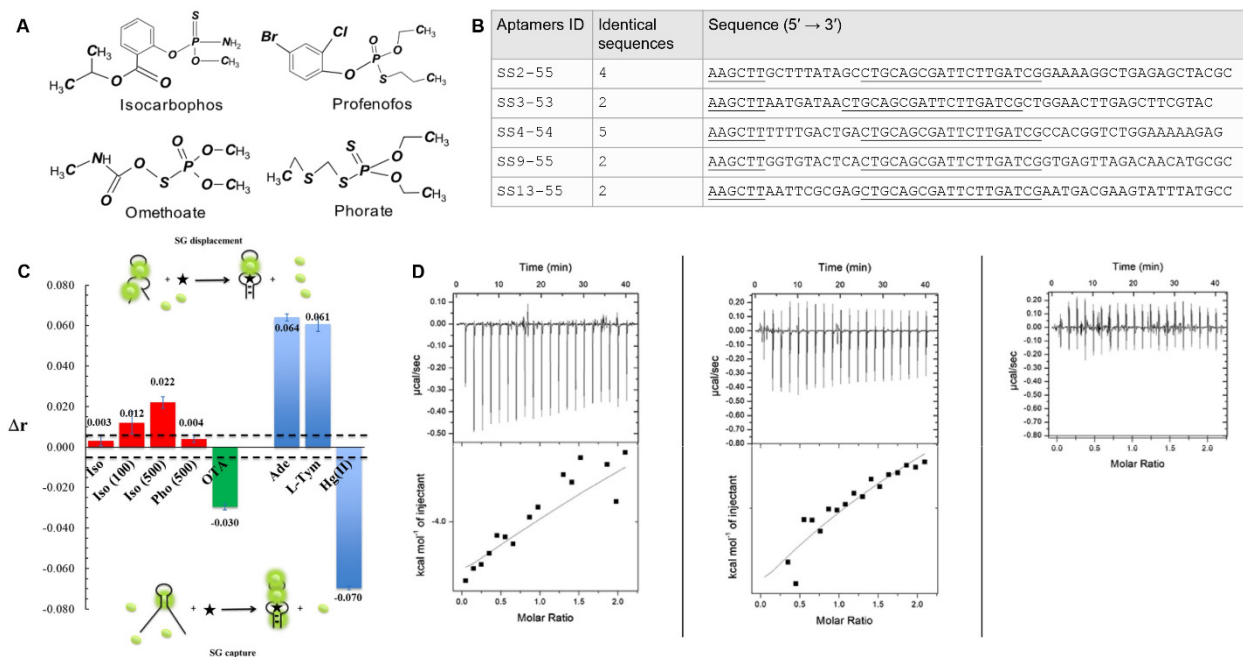
303 Aptamers have been selected for some of these pesticides, specifically isocarbophos,
 304 phorate, omethoate, and profenofos (Figure 7A). Although these four pesticides share some

305 similarity on the phosphate part, the structures are still vastly different, especially for the chemical
306 groups that can potentially interact with DNA. Nevertheless, Wang et al still used a mixture of
307 these four pesticides as targets, and a few DNA sequences were selected using the library
308 immobilized selection after 12 rounds of selection [67]. The degree of alignment of the random
309 region appeared to be low (Figure 7B). The authors developed a molecular beacon based
310 competitive assay, where the aptamers could bind to either their targets or hybridize with the
311 beacon. Among them, SS2-55 and SS4-54 were found to have the highest binding affinity to
312 isocarbophos. For these two sequences, the authors measured the K_d to be between 0.8 to 2.5 μM
313 for all the four pesticide molecules. This is a surprising result since the four pesticides are quite
314 different, and the common part with two methyl groups attached to the phosphate is unlikely to
315 interact with DNA with low micromolar affinity, since only very weak van der Waals forces can
316 act in this case. For comparison, the adenosine binding aptamer uses π - π stacking and hydrogen
317 bonding only to achieve a K_d of $\sim 6 \mu\text{M}$ [13, 29]. A subsequent work performed rational aptamer
318 truncation studies based on their secondary structures [68]. Although the title of this paper claimed
319 the use of fluorescence polarization, the method was still based on the molecular beacon
320 fluorescence intensity.

321 When these aptamers were more carefully scrutinized, it was recently found that they did
322 not respond to the presence of the pesticides to the degree that had been previously reported. For
323 example, when attempting to develop an aptasensor based on fluorescence anisotropy, the selected
324 aptamers were unable to interact with the pesticides even at very high concentrations [69]. Even
325 though the method of using fluorescence anisotropy (r) to assay target analyte binding has been
326 successfully employed in the past with hairpin [70], G-quadruplex [71], and unknown aptamer
327 structures [72]. Figure 7C shows the discrepancy between the changes in the Δr value of the
328 supposed aptamers for organophosphate pesticides and other small molecule aptamers from the
329 literature [73]. Δr values were calculated based on the release or capture of the SG dye upon
330 binding with the target. Compared to the ochratoxin aptamer (as a positive control) and the values
331 of the other aptamers in the literature, no significant interaction was detected between the
332 organophosphate aptamers and their intended pesticide targets.

333 ITC further confirmed this conclusion. Figure 7D (the first two traces) shows the ITC traces
334 generated when the SS2-55 and SS24-35 are titrated with isocarbophos, compared to the titration

335 of just buffer with isocarbophos (Figure 7D, the third trace). The aptamers only show a very small
 336 heat change, inconsistent with the reported dissociation constants. In this way, these traces could
 337 explain the lack of fluorescence anisotropy output upon the binding of the target.



338
 339 **Figure 7.** The structures of the four pesticides used as a mixture for the selection. (B) Sequence
 340 alignment of the selected aptamers. The underlined regions were the constant nucleotides and the
 341 others were randomized. Figure adapted from ref. [68] with permission. Copyright 2014 Elsevier.
 342 (D) ITC traces of SS2-55 (left), SS24-35 (middle), and buffer (right) titrated with isocarbophos. (C)
 343 Changes in Δr values of SS2-55 (Iso with isocarbophos), and SS24-35 (Iso(100), Iso(500), and
 344 Pho(500) for 100, 500 μ M of isocarbophos respectively, and 500 μ M of phorate), the ochratoxin
 345 A aptamer, and values of other small molecule aptamers in the literature. (A, B) Adapted from
 346 ref.[67] with permission. Copyright 2012 Springer. (C, D) Adapted from ref. [69] with permission.
 347 Copyright 2021 Elsevier.

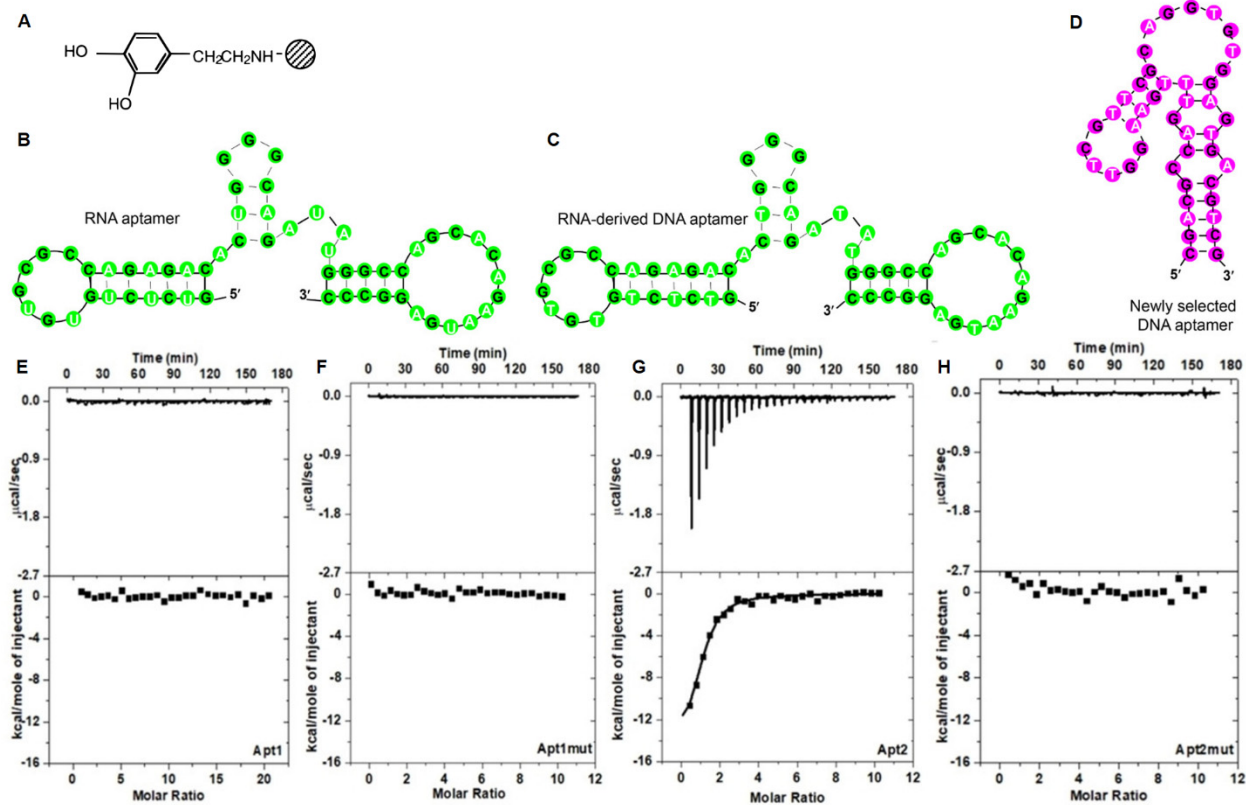
348
 349 **Dopamine**

350 Dopamine is a key neurotransmitter and its detection has attracted the attention of many
 351 researchers [74]. An RNA aptamer for dopamine was reported by Mannironi et al. in 1997 by
 352 immobilizing dopamine on a column via its primary amine (Figure 8A) [75]. After 9 rounds of

353 selection, the library was sequenced. Out of the 44 obtained sequences, there were 14 unique ones,
354 but sequence alignment among them was poor. The most abundant sequence was further analyzed
355 after alkaline hydrolysis to determine its minimal binding structure as shown in Figure 8B. The
356 binding was measured via affinity column elution, and the RNA aptamer had a K_d of 2.8 μ M.
357 Extensive mutation studies were performed to confirm specific binding and seven analog
358 molecules were tested to confirm selectivity. While this RNA aptamer was used for designing
359 biosensors [76], it's application was limited due to poor stability and high cost of RNA. As such,
360 a DNA aptamer for dopamine would be highly desirable.

361 An interesting attempt was made to simply convert the RNA sequence to DNA (Figure 8C),
362 and it was reported that this DNA analog could still bind dopamine [77]. Most of the aptamer-
363 based dopamine sensing work then used this RNA-derived DNA. However, an electrochemical
364 characterization argued against the selective dopamine binding ability of this DNA aptamer [78].
365 Recently, a new selection was performed using the library immobilization method (Figure 8D)
366 [23], and this aptamer demonstrated good binding affinity based on ITC measurements [79]. A
367 subsequent side-by-side comparison of the two DNA aptamers also failed to show the binding of
368 the RNA-derived DNA aptamer [80]. For example, Figures 8E and 8F are the ITC traces of the
369 RNA-derived aptamer and a mutant of it, neither of which showed binding. Figure 8G is the newly
370 selected DNA aptamer, which demonstrated strong binding of dopamine. Mutating key nucleotides
371 in this aptamer abolished the binding activity (Figure 8H).

372 The binding of the RNA-derived aptamer was only characterized by fluorescence
373 anisotropy, taking advantage of the fluorescence of dopamine [77]. However, it was pointed out
374 that the starting anisotropy values were too high for dopamine, suggesting potential artifacts in the
375 measurement [80]. Based on the literature survey, it is likely that dopamine binding to this RNA-
376 derived DNA aptamer is nonspecific.



377

378 **Figure 8.** (A) The immobilized dopamine used for the selection of its RNA aptamer. Figure
 379 adapted from ref. [75] with permission. Copyright 1997 American Chemical Society. The
 380 predicted secondary structures of (B) the RNA aptamer, (C) the RNA-derived DNA aptamer, and
 381 (D) the newly selected DNA aptamer using the library immobilization method. ITC traces of
 382 titrating dopamine into (E) the RNA-derived aptamer, and (F) its mutant, and (G) the newly
 383 selected DNA aptamer, and (H) its mutant. Figures adapted from ref. [80] with permission.
 384 Copyright 2021 Wiley-VCH GmbH.

385

386

387 Possible reasons for obtaining non-aptamers

388 The above sections reviewed five examples of small molecule binding DNA aptamers. Although
 389 most of them have been extensively used in biosensor design, rigorous binding assays indicated a
 390 lack of specific binding in each case. Aptamer binding is the basis of all subsequent bioanalytical
 391 applications. Aptamers need careful biochemical characterization including truncation and

392 mutation to optimize and confirm binding. As more labs have started to carry out aptamer selection
393 experiments, and more and more aptamers have been reported, rigorous binding assays have
394 lagged behind. We believe that a gap exists between aptamer selection and biosensor design. This
395 gap is the characterization of aptamers. In this section, we analyze possible reasons leading to non-
396 binding aptamers.

397 First, as discussed in the aptamer selection section, all selections can eventually generate
398 sequences in the final library, but the sequences could be due to nonspecific binding. Most of the
399 above aptamers were generated using the target immobilization method. However, the selection
400 libraries were also exposed to beads and test tubes, in addition to the immobilized target. Therefore,
401 if the target density was not sufficiently high, and the library was not subjected to stringent counter
402 selections against the beads and tubes, it is quite possible that the library could bind to these
403 surfaces instead of the target. Some target analytes, especially metal ions, are difficult to
404 immobilize. Although Ni^{2+} and Zn^{2+} were immobilized by chelators for aptamer selection [81, 82],
405 those RNA aptamers have yet to be used to design biosensors and few follow up works used them.
406 Arsenic is another example, as its immobilized state was quite different from the inorganic arsenic
407 used for detection [34]. Additional problems can arise from preferential amplification of certain
408 sequences during PCR [83]. All these factors may lead to the enrichment of non-aptamer sequences.
409 Fortunately, such problems can be identified by sequence alignment, as non-specific binding to
410 surfaces would likely result in random and poorly-aligned sequences [84]. Further confirmation
411 would then come from the binding assays.

412 Second, compared to antibodies, the types of binding assays for aptamers are far more
413 versatile [16, 17]. Many of the assays were derived from biosensors. However, not all assays are
414 reliable for all target analytes and are sometimes susceptible to artifacts. For example, using citrate-
415 capped AuNPs as a binding assay for newly selected aptamers could be problematic. Analytes that
416 can adsorb onto the gold surface would interfere with both the stability of AuNPs and the
417 adsorption of aptamers [18]. Without carefully designed control experiments to test these potential
418 artifacts, such assays alone would be insufficient to validate aptamers. We have analyzed some
419 As(III) sensors and believed that the use of AuNPs or gold surfaces could be a key reason for the
420 observed signals.

421

422 **Conclusions and future perspectives**

423 In this paper, we reviewed a few recent works claiming that some aptamers could not bind to their
424 targets. It is interesting that such scrutiny came quite late. This is probably due to a few reasons.
425 Firstly, it's more difficult to demonstrate non-binding than binding: many more techniques, under
426 a diverse range of buffer conditions, and aptamer/target concentration ranges, need to be carried
427 out to disprove an aptamer. Such work might be originated from careful control experiments or
428 the development of new biosensing methods, where the expected results could not be obtained. In
429 most cases, such projects might be abandoned without publishing the negative results.
430 Nevertheless, based on some recently published papers, we can ascertain that publication is
431 certainly possible. We recommend that works are re-examined for binding instead of attempting
432 to obtain some concentration-dependent signals. Although reporting a sequence that cannot bind
433 to the intended target, does not seem to add new knowledge, such works are also valuable, since
434 they can prevent further misleading and confusion in the field. Such reports can also encourage
435 new efforts to obtain working aptamers.

436 We expect more works to revisit other aptamers and test their binding, especially those
437 without previous systematic binding assays (e.g. ITC, truncation studies and test of mutants). For
438 most newly selected aptamers, only using AuNPs or DNA staining dyes to perform label-free
439 assays is insufficient. In addition, the majority of the aptamers discussed here were obtained from
440 target immobilization. We expect more work to be done on the library immobilization method [27].
441 For example, a high quality dopamine aptamer was obtained via the library immobilization method
442 [23]. In addition, aptamers for many sugars, neurotransmitters, and illicit drugs were also obtained
443 using this method [23, 25, 85]. We expect that many other molecules can also be selected using
444 this method. It would also be interesting to have more side-by-side comparisons between these
445 two selection methods. Finally, all the examples reviewed here are small molecules. Further work
446 might be carried out to validate protein binding aptamers as well.

447

448 **Acknowledgement**

449 Funding for this work was from the Natural Sciences and Engineering Research Council of Canada
450 (NSERC).

451 **References**

- 452 [1] C. Tuerk; L. Gold, Systematic evolution of ligands by exponential enrichment: RNA
453 ligands to bacteriophage T4 DNA polymerase, *Science* 249 (1990) 505-510.
- 454 [2] A. D. Ellington; J. W. Szostak, In vitro selection of RNA molecules that bind specific
455 ligands, *Nature* 346 (1990) 818-822.
- 456 [3] W. H. Tan; M. J. Donovan; J. H. Jiang, Aptamers from cell-based selection for
457 bioanalytical applications, *Chem. Rev.* 113 (2013) 2842-2862. 10.1021/cr300468w.
- 458 [4] E. M. McConnell; J. Nguyen; Y. Li, Aptamer-based biosensors for environmental
459 monitoring, *Front. Chem.* 8 (2020). 10.3389/fchem.2020.00434.
- 460 [5] H. Yu; O. Alkhamis; J. Canoura; Y. Liu; Y. Xiao, Advances and challenges in small-
461 molecule DNA aptamer isolation, characterization, and sensor development, *Angew. Chem. Int.*
462 *Ed.* 60 (2021) 16800-16823. <https://doi.org/10.1002/anie.202008663>.
- 463 [6] Q. Zhou; D. P. Tang, Recent advances in photoelectrochemical biosensors for analysis of
464 mycotoxins in food, *TrAC Trends Anal. Chem.* 124 (2020) 115814. 115814
10.1016/j.trac.2020.115814.
- 465 [7] P. Rothlisberger; M. Hollenstein, Aptamer chemistry, *Adv. Drug Delivery Rev.* 134
466 (2018) 3-21. 10.1016/j.addr.2018.04.007.
- 468 [8] Y. Wu; I. Belmonte; K. S. Sykes; Y. Xiao; R. J. White, Perspective on the future role of
469 aptamers in analytical chemistry, *Anal. Chem.* 91 (2019) 15335-15344.
470 10.1021/acs.analchem.9b03853.
- 471 [9] J. Liu; Z. Cao; Y. Lu, Functional nucleic acid sensors, *Chem. Rev.* 109 (2009) 1948–
472 1998.
- 473 [10] A. Ruscito; M. C. DeRosa, Small-molecule binding aptamers: Selection strategies,
474 characterization, and applications, *Front. Chem.* 4 (2016) 14. 10.3389/fchem.2016.00014.
- 475 [11] O. Alkhamis; J. Canoura; H. X. Yu; Y. Z. Liu; Y. Xiao, Innovative engineering and
476 sensing strategies for aptamer-based small-molecule detection, *TrAC-Trends Anal. Chem.* 121
477 (2019) 115699. 115699. 10.1016/j.trac.2019.115699.
- 478 [12] A. Roth; R. R. Breaker, The structural and functional diversity of metabolite-binding
479 riboswitches, *Annu. Rev. Biochem.* 78 (2009) 305-334.
480 10.1146/annurev.biochem.78.070507.135656.
- 481 [13] D. E. Huizenga; J. W. Szostak, A DNA aptamer that binds adenosine and ATP,
482 *Biochemistry* 34 (1995) 656-665.
- 483 [14] M. N. Stojanovic; P. de Prada; D. W. Landry, Aptamer-based folding fluorescent sensor
484 for cocaine, *J. Am. Chem. Soc.* 123 (2001) 4928-4931.
- 485 [15] L. C. Bock; L. C. Griffin; J. A. Latham; E. H. Vermaas; J. J. Toole, Selection of single-
486 stranded DNA molecules that bind and inhibit human thrombin, *Nature* 355 (1992) 564-566.
- 487 [16] M. McKeague; A. De Girolamo; S. Valenzano; M. Pascale; A. Ruscito; R. Velu; N. R.
488 Frost; K. Hill; M. Smith; E. M. McConnell; M. C. DeRosa, Comprehensive analytical
489 comparison of strategies used for small molecule aptamer evaluation, *Anal. Chem.* 87 (2015)
490 8608-8612. 10.1021/acs.analchem.5b02102.
- 491 [17] E. Daems; G. Moro; R. Campos; K. De Wael, Mapping the gaps in chemical analysis for
492 the characterisation of aptamer-target interactions, *TrAC, Trends Anal. Chem.* 142 (2021)
493 116311. <https://doi.org/10.1016/j.trac.2021.116311>.

494 [18] F. Zhang; J. Liu, Label-free colorimetric biosensors based on aptamers and gold
495 nanoparticles: A critical review, *Anal. Sens.* 1 (2021) 30-43.
496 <https://doi.org/10.1002/anse.202000023>.
497 [19] R. Nutiu; Y. Li, Structure-switching signaling aptamers: Transducing molecular
498 recognition into fluorescence signaling, *Chem. Eur. J.* 10 (2004) 1868-1876.
499 [20] R. Nutiu; Y. Li, Structure-switching signaling aptamers, *J. Am. Chem. Soc.* 125 (2003)
500 4771-4778.
501 [21] R. Nutiu; Y. Li, In vitro selection of structure-switching signaling aptamers, *Angew.*
502 *Chem. Int. Ed.* 44 (2005) 1061-1065.
503 [22] M. Rajendran; A. D. Ellington, Selection of fluorescent aptamer beacons that light up in
504 the presence of zinc, *Anal. Bioanal. Chem.* 390 (2008) 1067-1075.
505 [23] N. Nakatsuka; K.-A. Yang; J. M. Abendroth; K. M. Cheung; X. Xu; H. Yang; C. Zhao;
506 B. Zhu; Y. S. Rim; Y. Yang; P. S. Weiss; M. N. Stojanović; A. M. Andrews, Aptamer-field-
507 effect transistors overcome debye length limitations for small-molecule sensing, *Science* 362
508 (2018) 319-324. 10.1126/science.aao6750.
509 [24] K.-A. Yang; R. Pei; M. N. Stojanovic, In vitro selection and amplification protocols for
510 isolation of aptameric sensors for small molecules, *Methods* 106 (2016) 58-65.
511 <https://doi.org/10.1016/j.ymeth.2016.04.032>.
512 [25] W. J. Yang; H. X. Yu; O. Alkhamis; Y. Z. Liu; J. Canoura; F. F. Fu; Y. Xiao, In vitro
513 isolation of class-specific oligonucleotide-based small-molecule receptors, *Nucleic Acids Res.*
514 47 (2019). e71. 10.1093/nar/gkz224.
515 [26] H. X. Yu; W. J. Yang; O. Alkhamis; J. Canoura; K. A. Yang; Y. Xiao, In vitro isolation
516 of small-molecule-binding aptamers with intrinsic dye-displacement functionality, *Nucleic Acids*
517 *Res.* 46 (2018). 10.1093/nar/gky026.
518 [27] C. Lyu; I. M. Khan; Z. Wang, Capture-selex for aptamer selection: A short review,
519 *Talanta* 229 (2021) 122274. <https://doi.org/10.1016/j.talanta.2021.122274>.
520 [28] T. Schütze; B. Wilhelm; N. Greiner; H. Braun; F. Peter; M. Mörl; V. A. Erdmann; H.
521 Lehrach; Z. Konthur; M. Menger; P. F. Arndt; J. Glöckler, Probing the selex process with next-
522 generation sequencing, *PLoS ONE* 6 (2011) e29604. 10.1371/journal.pone.0029604.
523 [29] C. H. Lin; D. J. Patel, Structural basis of DNA folding and recognition in an AMP-DNA
524 aptamer complex: Distinct architectures but common recognition motifs for DNA and RNA
525 aptamers complexed to AMP, *Chem. Biol.* 4 (1997) 817-832.
526 [30] S. Shen; X.-F. Li; W. R. Cullen; M. Weinfeld; X. C. Le, Arsenic binding to proteins,
527 *Chem. Rev.* 113 (2013) 7769-7792. 10.1021/cr300015c.
528 [31] L. Zhang; X. R. Chen; S. H. Wen; R. P. Liang; J. D. Qiu, Optical sensors for inorganic
529 arsenic detection, *TrAC Trends Anal. Chem.* 118 (2019) 869-879. 10.1016/j.trac.2019.07.013.
530 [32] S. Kempahanumakkagari; A. Deep; K.-H. Kim; S. Kumar Kailasa; H.-O. Yoon,
531 Nanomaterial-based electrochemical sensors for arsenic - a review, *Biosens. Bioelectron.* 95
532 (2017) 106-116. <https://doi.org/10.1016/j.bios.2017.04.013>.
533 [33] C. Zong; X. Jin; J. Liu, Critical review of bio/nano sensors for arsenic detection, *Trends*
534 *Environ. Anal. Chem.* 32 (2021) e00143. <https://doi.org/10.1016/j.teac.2021.e00143>.
535 [34] M. Kim; H. J. Um; S. Bang; S. H. Lee; S. J. Oh; J. H. Han; K. W. Kim; J. Min; Y. H.
536 Kim, Arsenic removal from vietnamese groundwater using the arsenic-binding DNA aptamer,
537 *Environ. Sci. Technol.* 43 (2009) 9335-9340. 10.1021/es902407g.

538 [35] C. Zong; J. Liu, The arsenic-binding aptamer cannot bind arsenic: Critical evaluation of
539 aptamer selection and binding, *Anal. Chem.* 91 (2019) 10887-10893.
540 10.1021/acs.analchem.9b02789.

541 [36] H. Kimura-Suda; D. Y. Petrovykh; M. J. Tarlov; L. J. Whitman, Base-dependent
542 competitive adsorption of single-stranded DNA on gold, *J. Am. Chem. Soc.* 125 (2003) 9014-
543 9015. 10.1021/ja035756n.

544 [37] B. Liu; J. Liu, Interface driven hybrid materials based on DNA-functionalized gold
545 nanoparticles, *Matter* 1 (2019) 825-847.

546 [38] Y. Wu; S. Zhan; F. Wang; L. He; W. Zhi; P. Zhou, Cationic polymers and aptamers
547 mediated aggregation of gold nanoparticles for the colorimetric detection of arsenic(III) in
548 aqueous solution, *Chem. Commun.* 48 (2012) 4459-4461. 10.1039/c2cc30384a.

549 [39] Y. Wu; L. Liu; S. Zhan; F. Wang; P. Zhou, Ultrasensitive aptamer biosensor for
550 arsenic(III) detection in aqueous solution based on surfactant-induced aggregation of gold
551 nanoparticles, *Analyst* 137 (2012) 4171-4178. 10.1039/c2an35711a.

552 [40] K. Matsunaga; Y. Okuyama; R. Hirano; S. Okabe; M. Takahashi; H. Satoh, Development
553 of a simple analytical method to determine arsenite using a DNA aptamer and gold
554 nanoparticles, *Chemosphere* 224 (2019) 538-543.
555 <https://doi.org/10.1016/j.chemosphere.2019.02.182>.

556 [41] D. Zhang; Y. Liu; J. Ding; K. Hayat; X. Zhan; P. Zhou; D. Zhang, Label-free
557 colorimetric assay for arsenic(III) determination based on a truncated short ssDNA and gold
558 nanoparticles, *Microchimica Acta* 188 (2021) 38. 10.1007/s00604-020-04697-7.

559 [42] F. Yeasmin Khusbu; X. Zhou; H. Chen; C. Ma; K. Wang, Thioflavin T as a fluorescence
560 probe for biosensing applications, *TrAC Trends Anal. Chem.* 109 (2018) 1-18.
561 <https://doi.org/10.1016/j.trac.2018.09.013>.

562 [43] O. Suss; L. Motiei; D. Margulies, Broad applications of thiazole orange in fluorescent
563 sensing of biomolecules and ions, *Molecules* 26 (2021) 2828.

564 [44] N. L. Thao Nguyen; C. Y. Park; J. P. Park; S. K. Kailasa; T. J. Park, Synergistic
565 molecular assembly of an aptamer and surfactant on gold nanoparticles for the colorimetric
566 detection of trace levels of As³⁺ ions in real samples, *New J. Chem.* 42 (2018) 11530-11538.
567 10.1039/c8nj01097h.

568 [45] H. Li; L. J. Rothberg, Label-free colorimetric detection of specific sequences in genomic
569 DNA amplified by the polymerase chain reaction, *J. Am. Chem. Soc.* 126 (2004) 10958-10961.

570 [46] H. Li; L. Rothberg, Colorimetric detection of DNA sequences based on electrostatic
571 interactions with unmodified gold nanoparticles, *Proc. Natl. Acad. Sci. USA* 101 (2004) 14036-
572 14039.

573 [47] F. Zhang; P.-J. J. Huang; J. Liu, Sensing adenosine and atp by aptamers and gold
574 nanoparticles: Opposite trends of color change from domination of target adsorption instead of
575 aptamer binding, *ACS Sensors* 5 (2020) 2885-2893. 10.1021/acssensors.0c01169.

576 [48] C. Zong; Z. Zhang; B. Liu; J. Liu, Adsorption of arsenite on gold nanoparticles studied
577 with DNA oligonucleotide probes, *Langmuir* 35 (2019) 7304-7311.
578 10.1021/acs.langmuir.9b01161.

579 [49] K. Vega-Figueroa; J. Santillán; V. Ortiz-Gómez; E. O. Ortiz-Quiles; B. A. Quiñones-
580 Colón; D. A. Castilla-Casadiago; J. Almodóvar; M. J. Bayro; J. A. Rodríguez-Martínez; E.
581 Nicolau, Aptamer-based impedimetric assay of arsenite in water: Interfacial properties and
582 performance, *ACS Omega* 3 (2018) 1437-1444. 10.1021/acsomega.7b01710.

583 [50] M. Yuan; Q. Zhang; Z. Song; T. Ye; J. Yu; H. Cao; F. Xu, Piezoelectric arsenite
584 aptasensor based on the use of a self-assembled mercaptoethylamine monolayer and gold
585 nanoparticles, *Microchimica Acta* 186 (2019) 268. 10.1007/s00604-019-3373-1.

586 [51] B. Yang; X. Chen; R. Liu; B. Liu; C. Jiang, Target induced aggregation of modified
587 Au@Ag nanoparticles for surface enhanced raman scattering and its ultrasensitive detection of
588 arsenic(III) in aqueous solution, *RSC Advances* 5 (2015) 77755-77759. 10.1039/c5ra15954g.

589 [52] L. Song; K. Mao; X. Zhou; J. Hu, A novel biosensor based on Au@Ag core-shell
590 nanoparticles for sers detection of arsenic (III), *Talanta* 146 (2016) 285-290.
591 <https://doi.org/10.1016/j.talanta.2015.08.052>.

592 [53] M. Yuan; M. X. Wang; Y. Z. Zheng; H. Cao; F. Xu; T. Ye; J. S. Yu, Aptamer/gold
593 nanoparticles-based fluorometric and colorimetric dual-mode detection of arsenite, *Chin. J. Anal.*
594 *Chem.* 49 (2021) 76-84. 10.19756/j.issn.0253-3820.201180.

595 [54] K.-M. Song; E. Jeong; W. Jeon; M. Cho; C. Ban, Aptasensor for ampicillin using gold
596 nanoparticle based dual fluorescence-colorimetric methods, *Anal. Bioanal. Chem.* 402 (2012)
597 2153-2161. 10.1007/s00216-011-5662-3.

598 [55] M. A. D. Neves; S. Slavkovic; Z. R. Churcher; P. E. Johnson, Salt-mediated two-site
599 ligand binding by the cocaine-binding aptamer, *Nucleic Acids Res.* 45 (2016) 1041-1048.
600 10.1093/nar/gkw1294.

601 [56] L. Liu; L. Stepanian; D. N. Dubins; T. V. Chalikian, Binding of L-argininamide to a
602 DNA aptamer: A volumetric study, *J. Phys. Chem. B* 122 (2018) 7647-7653.
603 10.1021/acs.jpcc.8b03912.

604 [57] J. Zhou; Y. Li; W. Wang; Z. Lu; H. Han; J. Liu, Kanamycin adsorption on gold
605 nanoparticles dominates its label-free colorimetric sensing with its aptamer, *Langmuir* 36 (2020)
606 11490-11498. 10.1021/acs.langmuir.0c01786.

607 [58] F. Bottari; E. Daems; A.-M. de Vries; P. Van Wielendaele; S. Trashin; R. Blust; F.
608 Sobott; A. Madder; J. C. Martins; K. De Wael, Do aptamers always bind? The need for a
609 multifaceted analytical approach when demonstrating binding affinity between aptamer and low
610 molecular weight compounds, *J. Am. Chem. Soc.* 142 (2020) 19622-19630.
611 10.1021/jacs.0c08691.

612 [59] K.-M. Song; M. Cho; H. Jo; K. Min; S. H. Jeon; T. Kim; M. S. Han; J. K. Ku; C. Ban,
613 Gold nanoparticle-based colorimetric detection of kanamycin using a DNA aptamer, *Anal.*
614 *Biochem.* 415 (2011) 175-181. <https://doi.org/10.1016/j.ab.2011.04.007>.

615 [60] A. A. Yunis, Chloramphenicol toxicity - 25 years of research, *Am. J. Med.* 87 (1989)
616 N44-N48.

617 [61] J. Mehta; B. Van Dorst; E. Rouah-Martin; W. Herrebout; M.-L. Scippo; R. Blust; J.
618 Robbens, In vitro selection and characterization of DNA aptamers recognizing chloramphenicol,
619 *J. Biotechnol.* 155 (2011) 361-369. <https://doi.org/10.1016/j.jbiotec.2011.06.043>.

620 [62] L. Yan; C. Luo; W. Cheng; W. Mao; D. Zhang; S. Ding, A simple and sensitive
621 electrochemical aptasensor for determination of chloramphenicol in honey based on target-
622 induced strand release, *J. Electroanal. Chem.* 687 (2012) 89-94.
623 <https://doi.org/10.1016/j.jelechem.2012.10.016>.

624 [63] S. Wu; H. Zhang; Z. Shi; N. Duan; C. Fang; S. Dai; Z. Wang, Aptamer-based
625 fluorescence biosensor for chloramphenicol determination using upconversion nanoparticles,
626 *Food Control* 50 (2015) 597-604. <https://doi.org/10.1016/j.foodcont.2014.10.003>.

627 [64] S. K. Yadav; B. Agrawal; P. Chandra; R. N. Goyal, In vitro chloramphenicol detection in
628 a haemophilus influenza model using an aptamer-polymer based electrochemical biosensor,
629 Biosens. Bioelectron. 55 (2014) 337-342. <https://doi.org/10.1016/j.bios.2013.12.031>.

630 [65] X. Tao; F. He; X. Liu; F. Zhang; X. Wang; Y. Peng; J. Liu, Detection of chloramphenicol
631 with an aptamer-based colorimetric assay: Critical evaluation of specific and unspecific binding
632 of analyte molecules, Microchimica Acta 187 (2020) 668. 10.1007/s00604-020-04644-6.

633 [66] M. Liu; A. Khan; Z. Wang; Y. Liu; G. Yang; Y. Deng; N. He, Aptasensors for pesticide
634 detection, Biosens. Bioelectron. 130 (2019) 174-184. <https://doi.org/10.1016/j.bios.2019.01.006>.

635 [67] L. Wang; X. Liu; Q. Zhang; C. Zhang; Y. Liu; K. Tu; J. Tu, Selection of DNA aptamers
636 that bind to four organophosphorus pesticides, Biotechnol. Lett 34 (2012) 869-874.
637 10.1007/s10529-012-0850-6.

638 [68] C. Zhang; L. Wang; Z. Tu; X. Sun; Q. He; Z. Lei; C. Xu; Y. Liu; X. Zhang; J. Yang; X.
639 Liu; Y. Xu, Organophosphorus pesticides detection using broad-specific single-stranded DNA
640 based fluorescence polarization aptamer assay, Biosens. Bioelectron. 55 (2014) 216-219.
641 <https://doi.org/10.1016/j.bios.2013.12.020>.

642 [69] L. Zara; S. Achilli; B. Chovelon; E. Fiore; J.-J. Toulmé; E. Peyrin; C. Ravelet, Anti-
643 pesticide DNA aptamers fail to recognize their targets with asserted micromolar dissociation
644 constants, Anal. Chim. Acta 1159 (2021) 338382. <https://doi.org/10.1016/j.aca.2021.338382>.

645 [70] E. Goux; Q. Lespinasse; V. Guieu; S. Perrier; C. Ravelet; E. Fiore; E. Peyrin,
646 Fluorescence anisotropy-based structure-switching aptamer assay using a peptide nucleic acid
647 (PNA) probe, Methods 97 (2016) 69-74. <https://doi.org/10.1016/j.ymeth.2015.09.018>.

648 [71] J. A. Cruz-Aguado; G. Penner, Fluorescence polarization based displacement assay for
649 the determination of small molecules with aptamers, Anal. Chem. 80 (2008) 8853-8855.
650 10.1021/ac8017058.

651 [72] Z. Zhu; T. Schmidt; M. Mahrous; V. Guieu; S. Perrier; C. Ravelet; E. Peyrin,
652 Optimization of the structure-switching aptamer-based fluorescence polarization assay for the
653 sensitive tyrosinamide sensing, Anal. Chim. Acta 707 (2011) 191-196.
654 <https://doi.org/10.1016/j.aca.2011.09.022>.

655 [73] A. Kidd; V. Guieu; S. Perrier; C. Ravelet; E. Peyrin, Fluorescence polarization biosensor
656 based on an aptamer enzymatic cleavage protection strategy, Analytical and Bioanalytical
657 Chemistry 401 (2011) 3229-3234. 10.1007/s00216-011-5434-0.

658 [74] X. Liu; J. Liu, Biosensors and sensors for dopamine detection, VIEW 2 (2020) 20200102.

659 [75] C. Mannironi; A. Di Nardo; P. Fruscoloni; G. P. Tocchini-Valentini, In vitro selection of
660 dopamine RNA ligands, Biochemistry 36 (1997) 9726-9734.

661 [76] E. Farjami; R. Campos; J. S. Nielsen; K. V. Gothelf; J. Kjems; E. E. Ferapontova, RNA
662 aptamer-based electrochemical biosensor for selective and label-free analysis of dopamine, Anal.
663 Chem. 85 (2013) 121-128. 10.1021/ac302134s.

664 [77] R. Walsh; M. C. DeRosa, Retention of function in the DNA homolog of the RNA
665 dopamine aptamer, Biochem. Biophys. Res. Commun. 388 (2009) 732-735.
666 <https://doi.org/10.1016/j.bbrc.2009.08.084>.

667 [78] I. Álvarez-Martos; E. E. Ferapontova, A DNA sequence obtained by replacement of the
668 dopamine RNA aptamer bases is not an aptamer, Biochem. Biophys. Res. Commun. 489 (2017)
669 381-385. <https://doi.org/10.1016/j.bbrc.2017.05.134>.

670 [79] X. Liu; Y. Hou; S. Chen; J. Liu, Controlling dopamine binding by the new aptamer for a
671 FRET-based biosensor, Biosens. Bioelectron. (2020) 112798.
672 <https://doi.org/10.1016/j.bios.2020.112798>.

673 [80] Y. Hou; J. Hou; X. Liu, Comparison of two DNA aptamers for dopamine using
674 homogeneous binding assays, *ChemBioChem* 22 (2021) 1948-1954.
675 <https://doi.org/10.1002/cbic.202100006>.
676 [81] J. Ciesiolka; J. Gorski; M. Yarus, Selection of an RNA domain that binds Zn^{2+} , *RNA* 1
677 (1995) 538-550.
678 [82] H. P. Hofmann; S. Limmer; V. Hornung; M. Sprinzl, Ni^{2+} -binding RNA motifs with an
679 asymmetric purine-rich internal loop and a G-A base pair, *RNA* 3 (1997) 1289-1300.
680 [83] T. Wang; C. Chen; L. M. Larcher; R. A. Barrero; R. N. Veedu, Three decades of nucleic
681 acid aptamer technologies: Lessons learned, progress and opportunities on aptamer development,
682 *Biotechnol. Adv.* 37 (2019) 28-50. <https://doi.org/10.1016/j.biotechadv.2018.11.001>.
683 [84] Y. Zhou; Z. Huang; R. Yang; J. Liu, Selection and screening of DNA aptamers for
684 inorganic nanomaterials, *Chem. Eur. J.* 24 (2018) 2525-2532. doi:10.1002/chem.201704600.
685 [85] K.-A. Yang; M. Barbu; M. Halim; P. Pallavi; B. Kim; D. M. Kolpashchikov; S. Pecic; S.
686 Taylor; T. S. Worgall; M. N. Stojanovic, Recognition and sensing of low-epitope targets via
687 ternary complexes with oligonucleotides and synthetic receptors, *Nat. Chem.* 6 (2014) 1003-
688 1008. 10.1038/nchem.2058.

689

690